Available online at www.sciencedirect.com
SCIENCE DIRECT®
Journal of Nuclear Materials 337–339 (2005) 400–404
journal of nuclear materials
www.elsevier.com/locate/jnucmat

Magnetic structure at the edge of a compact stellarator (NCSX)

A. Grossman [a,*], T. Kaiser [b], P.K. Mioduszewski [c]

[a] University of California San Diego, 9500 Gilman Drive, Mail Code 0417, La Jolla CA. 92093-0417, USA
[b] Lawrence Livermore National Laboratory, P.O. Box 808, Livermore, CA 94550, USA
[c] Oak Ridge National Laboratory, P.O. Box 2009, Oak Ridge TN 37831-8072, USA

Abstract

The magnetic field between the plasma surface and wall of the National Compact Stellarator (NCSX), is mapped via field line tracing in finite beta (4%) configurations with part (20%) of the rotational transform generated by the bootstrap current. The edge plasma magnetics are more stellarator-like, with a complex 3D structure, and less like the ordered 2D symmetric structure of a tokamak. The field lines make a transition from ergodically covering a surface to ergodically covering a volume, as the distance from the last closed magnetic surface is increased. The first few toroidal transits from the starting points are highly structured, with significant flux expansion at the bean shaped cross-section. The later toroidal transits become moderately stochastic, but with Kolmogorov lengths that can be made smaller than the connection if the separation between wall and plasma is sufficiently large.

PACS: 52.40.Hf; 52.55.Hc
Keywords: Magnetic topology; Stochastic boundary; Island divertor; Divertor

1. Introduction

Stellarators and tokamaks are both attractive approaches in magnetic confinement fusion. Tokamaks have demonstrated dramatic advances in performance, and physics understanding, as the 2D symmetry facilitates both analysis and construction. The stellarator uses 3D helical fields from coils to generate the rotational transform and provide an inherent divertor structure, thereby solving two major problems of tokamaks- disruptions and the achievement of steady state operation. However in standard stellarators the 3D shape implies that the particle orbits can have resonant perturbations, become stochastic, resulting in particles that are easily lost to the walls, requiring selection of large aspect ratios to ameliorate the resulting large transport. Two new strategies are available for improving orbit confinement in 3D and reducing the transport to the walls. These are the (1) drift-optimized stellarator (non-symmetric drift-orbit omnigeneity), in which the toroidal and helical drifts cancel and is the principle of the new W-7X stellarator, and (2) the quasi-symmetric stellarator, in which it is recognized that the drift orbits depends only on the variation of the magnitude of magnetic field within a flux surface and not on its vector components. By choosing a magnetic field magnitude which has axisymmetry, the stellarator configuration can have good

* Corresponding author. Tel.: +1 858 534 9712; fax: +1 858 534 7716.
E-mail address: agrossman@ferp.ucsd.edu (A. Grossman).

0022-3115/$ - see front matter © 2004 Elsevier B.V. All rights reserved.
doi:10.1016/j.jnucmat.2004.10.122

tokamak-like transport while still retaining a vector magnetic field that is 3D. Using this quasi-axisymmetry (QAS), a low aspect ratio configuration can be achieved which combines the best features of both the stellarator and tokamak, and is the basis for the National Compact Stellarator Experiment (NCSX) [1]. The 3D plasma geometry then allows access to degrees of freedom to achieve plasma properties that are not available in 2D configurations, such as the stabilization of instabilities without close fitting conducting walls or feedback. Rotational transform, shaping, and magnetic symmetry are thus available in this configuration as unique controls to understand the fundamentals of toroidal confinement and its relation to plasma performance, such as how islands and stochasticity affect the plasma boundary and plasma-material interactions. In NCSX control over power and particle handling is provided by controlled target surfaces, the location of which is governed by both practical issues and such as port locations and plasma performance issues [2,3]. To accommodate the 3D shaping of the plasma, the plasma facing components must also be 3D with an approximately conformal shape. One complication is that the ordered magnetic field structure found outside the separatrix of axisymmetric tokamaks is not necessarily present in the 3D edge of the stellarator plasma. The first and most basic task is then the determination of this topology for the compact QAS stellarator.

2. Magnetics methodology

We adopt the methodology developed for W7-X, in which an equilibrium solution is computed by an inverse equilibrium solver based on an energy minimizing variational moments code, VMEC2000 [4], which solves directly for the shape of the flux surfaces given the external coils and their currents as well as a bootstrap current provided by a separate transport calculation. The VMEC solution and the Biot-Savart vacuum fields are coupled to the magnetic field solver for finite-beta equilibrium (MFBE_2001) [5] code to determine the magnetic field on a three-dimensional grid over a computational domain (which is here selected to be a circle with radius sufficiently large to include the vacuum vessel and first wall.) VMEC yields Fourier coefficients of a number of discrete flux surfaces and of magnetic field on surfaces. MFBE transforms these results to its own curvilinear coordinates, the s, u, v system, where $s = 0$ at the magnetic axis and 1 at the plasma boundary. MFBE obtains values at arbitrary s by linear interpolation between neighboring flux surfaces. Outside of the boundary MFBE determines the magnetic field by integration of surface currents via the Shafranov virtual casing principle. To achieve high numerical accuracy, the number of integration points is adapted to the distance of the grid point from the plasma boundary, as this can be very small for some grid points, especially those associated with the scrape-off layer. This nonequidistant integration mesh is embedded in the equidistant one, and integration intervals are increased with distance from the plasma boundary up to the equidistant mesh used in the toroidal direction. The MFBE code is fully parallelized, so that the number of processors corresponds to the number of toroidal planes per period used in the calculation. The overall grid box has a rectangular cross-section and so may include many points that are far from the plasma boundary where knowledge of the magnetic field is not needed, so an outer boundary is introduced which can be conformal to the plasma boundary. For the cases presented here, this outer domain boundary is chosen to be circular. MFBE's output consists of the magnetic field everywhere on this circular domain, in a form which is suitable for field line tracing, which is a useful though not the most general technique for visualizing the complex 3D magnetic field. GOURDON codes are applied to this magnetic field to trace individual field lines with starting points specified relative to the LCMS calculated by VMEC and followed for a specified number of toroidal transits or until the domain boundary is reached.

3. Field line tracing results

Field line tracing has been performed for a number of NCSX configurations and tend to be qualitatively similar. The field line features most commonly observed may be seen in Fig. 1(a)–(d), which is the Poincare section data for the NCSX configuration m50_256, a multifilament model, at cross-sections in toroidal angles, 0°, 30°, 60° and 90°. Field lines are started at a series of equally spaced points incremented radially outwards from the LCMS as determined by VMEC. Each starting point is followed for a total of 200 toroidal transits, or until the line leaves the computational domain. The field lines do not form nested surfaces outside the LCMS, but make many toroidal revolutions close to it. Field lines launched within 1 cm outside of the LCMS generally do not exhibit much stochasticity, especially over the first few toroidal turns where they resemble the nested surfaces within the LCMS. This remains the case over a range of beta values, although there is a very rapid degradation of the the nested nature of the flux surfaces near the LCMS when island healing is not applied. The surfaces are ergodically covered (in the sense of densely covered). Closed field lines are found at the rational surfaces inside the plasma, for example $\iota = 0.6$, and such field lines explore only a fraction of the toroidal surface, while those away from these rational surfaces approach every point on the surface. When these iota values decrease back to 0.6 after crossing the LCMS, field lines

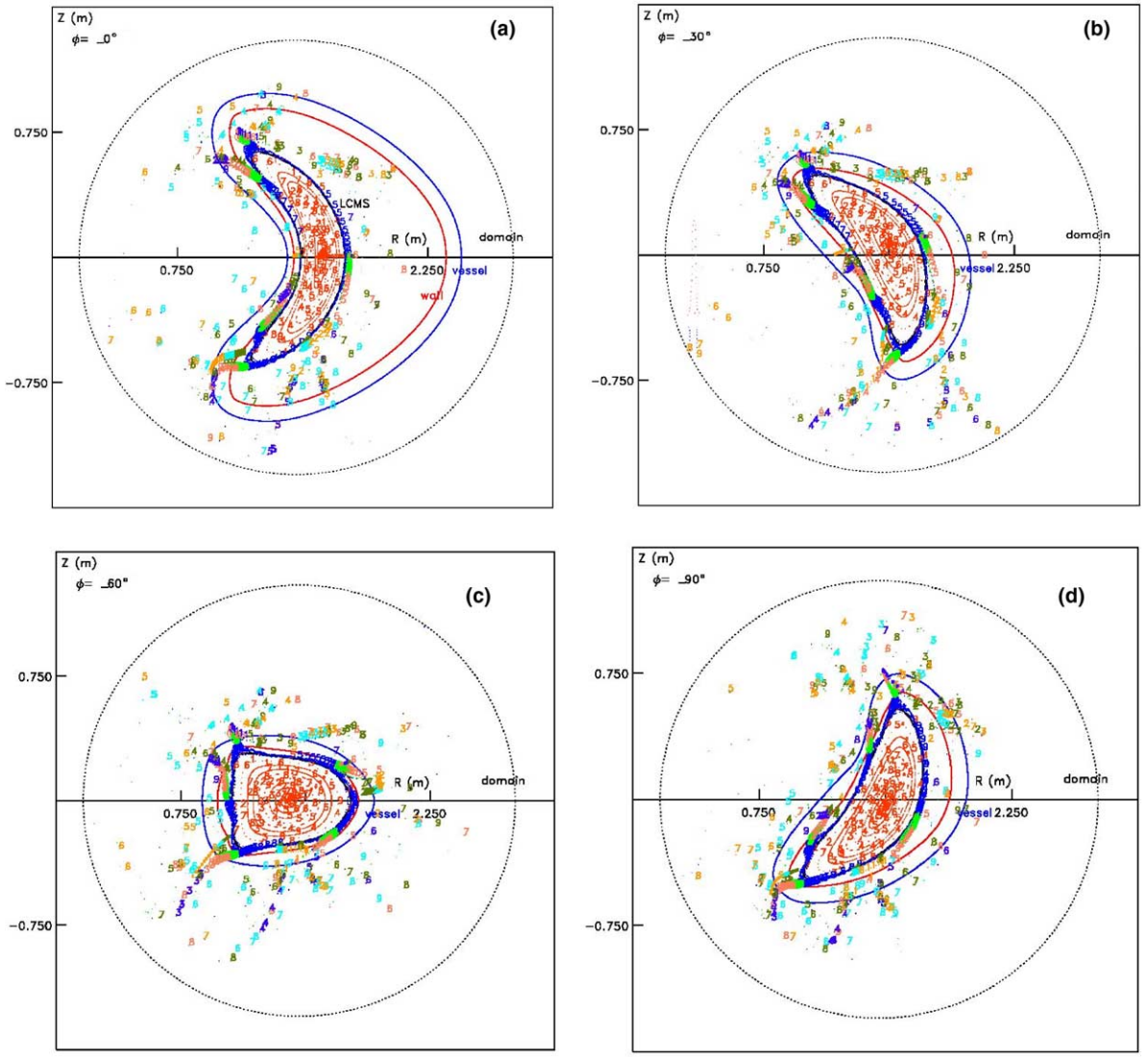

Fig. 1. Poincare puncture plot for NCSX configuration m50_256 multifilament coil model at (a) 0°, (b) 30°, (c) 60° and (d) 90° cross-sections.

are sometimes seen to form small 3/5 island chain. These closed lines are exceptional as small perturbations of currents can destroy their closure leaving island remnants. Further away from the LCMS, the field lines begin to travel over a volumetric region rather than a surface, and one has a flux volume rather than flux surface, over which field lines and particles freely travel. For regions close to the LCMS (within 1–2 cm), the flux volumes resemble surfaces of finite width, but as starting points of field lines are further out from the LCMS, the volumes become larger and less conformal to the shape of the LCMS. This chaotic threading of a 3D region, termed magnetic braiding by Stix [6] or stochasticity, not to be confused with the probability definition implying randomness [7]. These field lines are not random, they instead perform a very ordered expansion (near the tips of the bean shaped cross-section) during the first few toroidal transits, but also return to regions around the LCMS, before undergoing a much larger step that can bring them to circulate around separate external coils rather than around plasmas. The numbers adjacent to each point in these figures is the transit number in each period, '0' being the starting points (the horizontal series of 10 consecutive points over 1 cm radial extent from various positions on the outside LCMS at the 0° cross-section). The ordering of the field lines are preserved on these first few period transits, with ×5 flux expansion on the first period transit which can provide

inherent divertor action without the need for additional divertor coils. As this cross-section is the region where neutral beam injection occurs, the distance to the vacuum vessel is largest here. The plasma will initially be limited at ths 60° location, with limiter operation defined as PFCs which are in contact with the confined plasma and cutting what would otherwise be a closed surface. In the divertor mode of operation, the PFCs intercept open field lines only and there is an edge plasma between the main confined plasma and the PFC. The conformal wall armor at the 0° cross-section will serve as a kind of divertor baffle during the initial ohmic phase of the machine's operation. In later phases, the baffles will be optimized for recycling control and impurity control based on detailed neutral and impurity transport modeling which will eventually lead to an optimized divertor baffle with divertor pumping. Selected field lines are superimposed in the 3D model [8] of the NCSX plasma in Fig. 2. In this case the lines launched on the VMEC LCMS remain there, while lines launched further away, show a strong displacement and flux expansion near the helical edges that are most pronounced at the bean shaped cross-section, an inherent divertor that has been utilized in large aspect ratio stellarators. The resulting foot print giving the region of maximum interaction with external surfaces [3], is the basis of a stochastic field line divertor. An important quanitity is the degree of stochasticity, as measured by the Kolmogorov length and whether it is less than the connection length to the divertor plate. This is determined by following the correlation of nearby starting for many toroidal turns [9]. For field lines started close to the LCMS, the distance between the field lines grows exponentially with toroidal turns, as in Fig. 3(a). Many field lines exhibit a more complex behavior, especially when followed for a long period of time with oscillatory minima in their relative distance, indicative of differences in relative effective iota as shown in Fig. 3(b).

The VMEC representation assumes flux surfaces are simply connected without islands or stochastic regions.

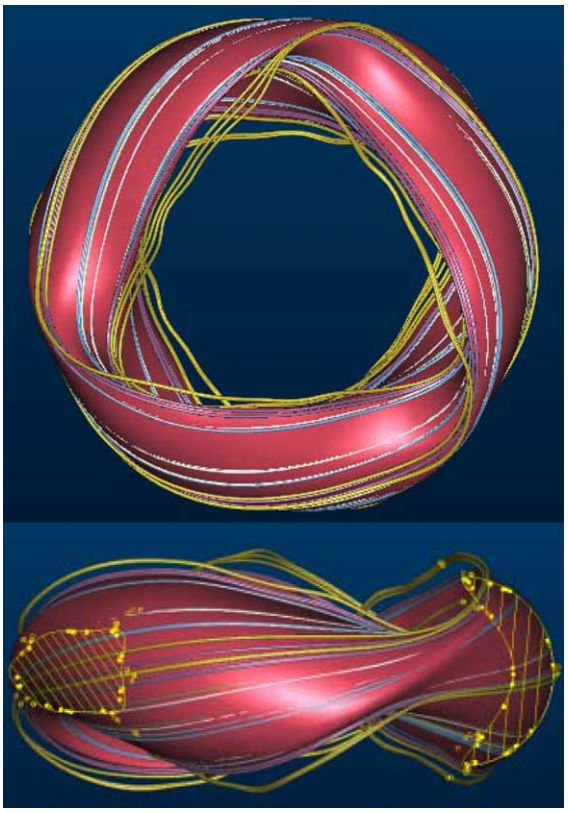

Fig. 2. Selected field lines from line-tracing superimposed on 3D model of the NCSX plasma.

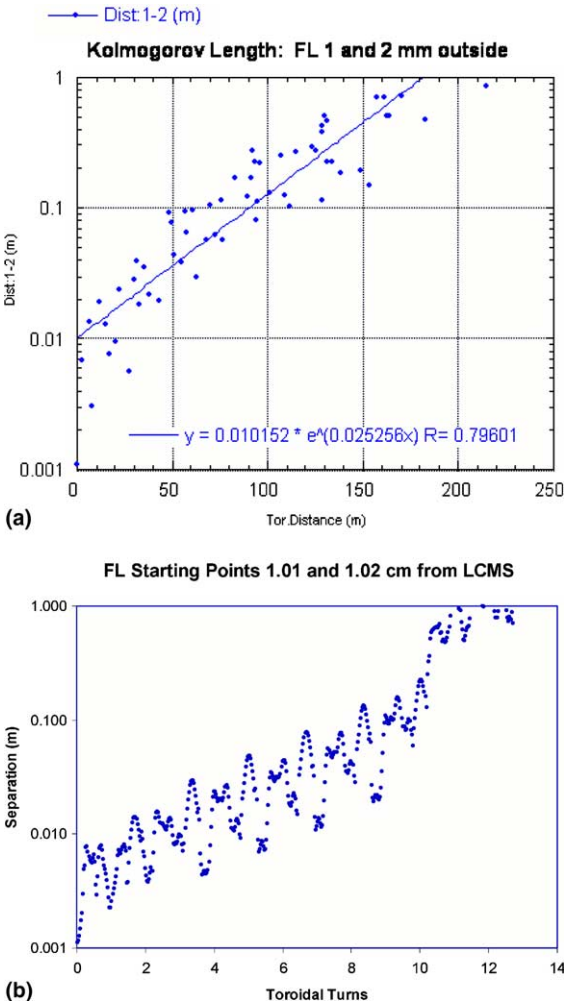

Fig. 3. Distance between field lines as a function of distance along field line, for determination of Kolmogorov lengths relative to connection length.

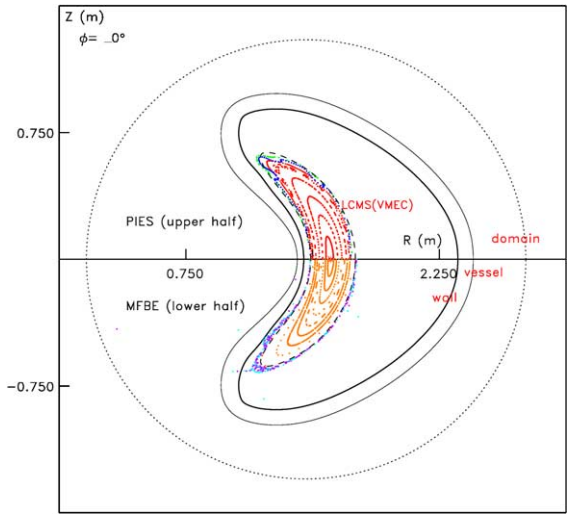

Fig. 4. Comparison of PIES 3D iterative MHD result (upper half plane) and VMEC-MFBE_2001-Gourdon field line tracing (lower half plane).

It is of interest to compare the results of this procedure with the results of PIES, a 'forward' equilibrium solver, which directly calculates 3D magnetic fields and current distributions, but simulates islands and stochastic regions by flattening pressure gradients. MFBE treats the zones around the LCMS differently depending on whether they are inside or outside the LCMS, using VMEC as well as direct 3D magnetics calculation to calculate islands and stochastic in regions near the LCMS, so a disagreement between MFBE LCMS and VMEC LCMS is possible and indicative of islands or stochastic regions inside the LCMS. Fig. 4 shows a PIES result for in the upper half plane and the VMEC result in the lower half. The PIES result has small islands within the LCMS and a significant distortion of the LCMS at the tips of the bean shaped cross-section.

4. Summary

The magnetic field inside and outside the plasma has been calculated for various QAS finite beta equilibria of NCSX. The fields are qualitatively similar, the ordered field line structure undergoes a transition from a flux surface to a flux volume with stochasticity on crossing the LCMS. Observations include an ×5 flux expansion near the tips of the bean shape that may be useful for inherent divertor, and stochastic regions and island remnants outside the LCMS, dependent on how island healing is applied and the range of iotas found near the LCMS.

References

[1] G.H. Neilson, M.C. Zarnstorff, L.P. Ku, E.A. Lazarus, P.K. Midouszewski, M. Fenstermacher, E. Fredrickson, G.Y. Fu, A. Grossman, et al., Physics Considerations in the Design of NCSX, PPPL-3753, October 2002.
[2] P. Mioduszewski, A. Grossman, et al., J. Nucl. Mater. 313 (2003) 1304.
[3] A.E. Koniges, A. Grossman, et al., J. Nucl. Fusion 43 (2003) 107.
[4] S.P. Hirshman et al., Comput. Phys. Commun. 43 (1986) 143.
[5] E. Strumberger et al., Nucl. Fusion 42 (2002) 827.
[6] T.H. Stix, Phys. Rev. Lett. 30 (1973) 833.
[7] R.D. Hazeltine, J.D. Meiss, Plasma Confinement, Addison Wesley, 1992.
[8] B. Nelson et al., 'NCSX In-vessel Design Update' NCSX Project Meeting, PPPL 28, August 2001.
[9] E. Strumberger, J. Nucl. Mat. 266–269 (1999) 1207.